

Mechanistic elucidation of the role of Salicylhydroxamic acid methyl ester in resistance of kiwifruit to *Botrytis cinerea*

Jiaqi Yang, Yijia Ma, Zhixin Li*, Hongpan Zhong, Xu Wang and Tianjing Zeng

Chongqing Key Laboratory for Germplasm Innovation of Special Aromatic Spice Plants, Collaborative Innovation Center of Special Plant Industry in Chongqing, College of Smart Agriculture/ Institute of Special Plants, Chongqing University of Arts and Sciences, Yongchuan 402160, China

* Corresponding author, E-mail: lizhexin_8903@163.com

Abstract

Kiwifruit (*Actinidia chinensis*) is a high-economic-value fruit crop cultivated worldwide. *Botrytis cinerea* infection, which causes *Botrytis cinerea* of kiwifruit after harvest, poses serious challenges to its production and storage. Salicylhydroxamic acid methyl ester (SHAM), an inhibitor of jasmonic acid synthesis, is involved in disease resistance in plants; however, its mechanism of action remains unclear. In this study, kiwifruit were infected with *Botrytis cinerea* after treatment with different concentrations of SHAM for 24 h. Treatment with an appropriate concentration of SHAM reduced the resistance of kiwifruit to *Botrytis cinerea*. After 0, 24, 48, and 120 h of *Botrytis cinerea* infection, fruit materials at the junction of disease and health were collected and analyzed using transcriptome sequencing. Differentially expressed genes with an FDR < 0.05 and $|\log_2FC| > 1$ were identified. Compared with the 0 h infection control group, 714, 1,511, and 4,181 differentially expressed genes were identified at 24, 48, and 96 h of infection, and most of the differentially expressed genes were regulated in the SHAM treatment group fruits. KEGG pathway analysis revealed that the related genes were mainly enriched for 'flavonoid biosynthesis', 'Phenylpropane biosynthesis', 'Mitogen-Activated Protein Kinase signal pathway', 'plant hormone signal transduction', and other metabolic pathways. These results unravel the molecular mechanism underlying the effect of SHAM in the resistance to *Botrytis cinerea* and provide an important basis for safe and efficient control of *Botrytis cinerea* in kiwifruit production.

Citation: Yang J, Ma Y, Li Z, Zhong H, Wang X, et al. 2024. Mechanistic elucidation of the role of Salicylhydroxamic acid methyl ester in resistance of kiwifruit to *Botrytis cinerea*. *Technology in Horticulture* 4: e026 <https://doi.org/10.48130/tihort-0024-0023>

Introduction

Kiwifruit (*Actinidia chinensis*), known as the 'King of fruits', has important economic, ecological, and social benefits. However, its susceptibility to fungal infection after harvest causes huge economic losses and poses potential safety concerns. *Botrytis cinerea*, caused by *Botrytis cinerea*, is one of the main postharvest diseases of kiwifruit, which can lead to a spoilage rate above 20%^[1].

Plant hormones^[2] are chemicals produced by plants, which, at low concentrations, affect their vital activities by regulating physiological processes, such as growth^[3], development, reproduction, and stress response. Jasmonic acid (JA)^[4] is a plant hormone closely related to plant resistance that plays an important role in plant growth, development, and stress response. It is widely regarded as a signaling molecule in plants that regulates physiological processes, such as disease resistance^[5], stress resistance^[6], flowering, and fruit ripening. JA also participates in plant defense response^[7]. Synthesis of JA in plants increases under unfavorable environments^[8], thereby promoting the initiation of defense mechanisms. Together with other plant hormones, JA regulates plant growth, development, and stress response^[9].

SHAM is an inhibitor of lipoxygenase (LOX), a key enzyme in the JA biosynthetic pathway^[10]. Therefore, SHAM may be involved in the regulation of plant responses to stress^[11–13]. In tomato, 5-aminolevulinic acid (ALA) was reported to enhance oxidative stress tolerance at low temperatures through the

nitric oxide (NO), JA, and hydrogen peroxide (H₂O₂) signaling pathways. Through plant culture, biochemical analysis, and gene expression studies, it was found that ALA pretreatment could enhance the activity of antioxidant enzymes in tomato and enhanced the tolerance to cold injury through a synergistic effect of JA and H₂O₂ and a downstream signaling effect of NO. These results indicated that ALA plays an important role in regulating the response of tomato^[14] to low temperatures, providing a potential molecular mechanism for improving the cold tolerance of crops. In *Brassica napus*^[15], the inhibitory effects of polyunsaturated fatty acids (PUFA) and methyl jasmonate (MeJA) on osmosis-induced proline accumulation were studied. PUFA and MeJA inhibited this accumulation, and MeJA exhibited an antagonistic effect on abscisic acid (ABA), a plant hormone that affects drought stress response by regulating proline metabolism. In a potato tuber formation study^[16], the effects of SHAM on theobromine-induced tuber formation, as well as on while endogenous JA and tubular acid (TA) levels and LOX activity, were investigated. SHAM inhibited theobromine-induced potato tuber formation, which is related to JA and TA biosynthesis and regulation of LOX activity. The effects of alternative oxidase (AOX) activity on phenol metabolism were investigated in MeJA-treated hairy root cultures of carrot^[17], employing the AOX inhibitors, SHAM and PG. AOX activity was positively correlated with phenylpropane biosynthesis, and MeJA enhanced the accumulation of phenolic acids, flavonoids, and lignin by upregulating AOX and phenylalanine

ammonia-lyase (PAL) activities. Moreover, in the endophytic fungus *Trichoderma atroviride* D16 from *Salvia miltiorrhiza*^[18], the effects of smoke-isolated butenolactone (KAR₁) on tanshinone I (T-I) production were investigated, and JA production and signal transduction were analyzed. KAR₁ increased the production of T-I by inducing the production of JA, which indicated the role of JA signaling in this process and provided valuable information for improving the content of medicinal ingredients.

The roles of SHAM in plant disease and defense have been extensively discussed. However, research on its effects as an exogenous activator on the postharvest disease of fruits is insufficient, and the mechanisms underlying its effects remain unclear. In this study, the effect of SHAM on *Botrytis cinerea* resistance in kiwifruit was investigated. We performed high-throughput transcriptome sequencing of SHAM-treated kiwifruit samples, enrichment analysis of differentially expressed genes (DEGs), and analysis of the main metabolic pathways affected by SHAM to unravel the molecular mechanisms involved. The present results provide potential strategies for the biocontrol of postharvest diseases and the promotion of sustainable agriculture.

Materials and methods

Kiwifruit material

Selected 'Red Yang' kiwifruit (*Actinidia chinensis* cv. Hongyang) were provided by Sanlei Tiantian Agricultural Development Co., Ltd., Chongqing, China (108.83° E, 29.59° N). 'Hongyang' kiwifruit exhibiting good shape, uniform size, and absence of pests and diseases were selected and transported to the laboratory within 6 h of harvesting. The fruits were disinfected by soaking in 2% sodium hypochlorite solution for 2 min, rinsed with disinfected distilled water, and dried at 25 °C for further use.

SHAM treatment and *Botrytis cinerea* infection

Ten microliter SHAM solution (0.1 mol/L) was injected into the pores of dried fruit, which were subsequently dried again. Thereafter, sterile water was injected three times and *Botrytis cinerea* (10⁴ spores/mL) was inoculated 24 h later. Diseased and healthy junction samples were collected at different time points (0, 24, 72, and 120 h, corresponding to S_{0h}, S_{24h}, S_{72h}, and S_{120h}, respectively) and diameters of the fungal lesions were determined using ImageJ software.

Total RNA extraction and transcriptome sequencing

The SHAM-treated kiwifruit were inoculated with *Botrytis cinerea* on day 0, 1, 3, and 5 in triplicate for each of the time points. Total RNA was extracted using a magnetic bead assay kit. The RNA samples were assessed for quality for use in the construction of cDNA library. Transcriptome sequencing was commissioned to Nanjing Ovisen Gene Technology Co., Ltd (Nanjing, China). The constructed library was initially quantified using a Qubit2.0 fluorometer, library insert size detection, and qRT-PCR. The qualified samples were sequenced on an Illumina platform. Finally, the PCR products were purified (AMPure XP system), and the library quality was assessed using an Agilent Bioanalyzer 2100 system. The raw RNA-seq data were deposited in the NCBI SRA database (Accession number: PRJNA1104815).

Quality control

Raw data (raw reads) in fastq format were first processed using in-house Perl scripts. In this step, clean data (clean reads) were obtained by removing the reads containing adapters, poly-N, and low-quality reads from the raw data. Simultaneously, the Q20, Q30, GC content and sequence duplication levels of the clean data were calculated. All downstream analyses were based on clean high-quality data, and adaptor sequences and low-quality sequence reads were removed from the datasets. The clean reads were mapped to the reference genome sequence using STAR. Only reads with a perfect match or one mismatch were further analyzed and annotated based on the reference genome. HTSeq (v 0.5.4) was used to count the number of reads mapped to each gene. Gene expression levels were estimated as fragments per kilobase of transcript per million mapped reads (FPKM).

Differential gene expression analysis

Differential gene expression analysis of two conditions or groups was performed using the DESeq R package (version 1.10.1). DESeq provides statistical routines for determining differential expression in digital gene expression data, using a model based on a negative binomial distribution. The resulting *p* values were adjusted using Benjamini and Hochberg's approach for controlling the false discovery rate (FDR). Genes with an adjusted *p*-value < 0.05 found using DESeq were assigned as differentially expressed. The sequence available at <http://kiwifruitgenome.org/> was used as the reference genome. Different infection times (0, 24, 72, and 120 h) were selected, and DEGs between the SHAM treatment and control groups (SHAM120h : CK120h) were identified based on the filtering criteria of false-discovery rate (FDR) < 0.05 and |log₂FC| greater than 1 and less than -1. A volcano plot was generated using the OmicShare tool to analyze the DEGs at different infection times (0, 24, 72, and 120 h). The Venn mapping tool was used to compare DEGs associated with *Botrytis cinerea*. These DEGs were subjected to the KEGG pathway enrichment analysis. The DEGs expression have been validated by qRT-PCR, and the primers used are listed in Table 1.

Table 1. Primers used in the present study.

Purpose	Gene ID		Primers (5'-3')
qRT-PCR	<i>β</i> -Actin	F	ACCGACATTTTCTGCAACC
		R	AGCAGCTGAGGTTGATCTGT
qRT-PCR	CEY00_Acc00618	F	CGTTGGGTTTGTGCTCTGAAA
		R	TCCTCAAACATGTCACCGGA
qRT-PCR	CEY00_Acc11227	F	CCCATAATCGAAAAGGCCGG
		R	TCACCAGATCGATCAGCCTC
qRT-PCR	CEY00_Acc16583	F	CTTGAACCACCGCAACTTGA
		R	CCTACGCATCTTCTCCAGT
qRT-PCR	CEY00_Acc20943	F	CTCCGGTGATCTGATCCCTCT
		R	ATTCCTAGTGCCAGGCCCTT
qRT-PCR	CEY00_Acc22367	F	CCGAGACTTTGTTGCTTGCTC
		R	CAGACCTCCCGATTCTCTC
qRT-PCR	CEY00_Acc23338	F	TTCCAACCTCTCCATCCAC
		R	GCCGATGATGGGTGAAGAAC
qRT-PCR	CEY00_Acc24966	F	ACTGGTCGTCTGCTCTGAAA
		R	GCCCCATCACTATCCGGTAA
qRT-PCR	CEY00_Acc27491	F	TTGTTTCAGTTGATGCAGGGCC
		R	AAACAGTGCACCCGAGTTTC
qRT-PCR	CEY00_Acc29568	F	ACCAGACTGCCATTCATGA
		R	GCACGGCTTTGTCAGATGAT

Statistical analyses

Statistical analyses were performed using SPSS 18.0. The Student's *t*-test was used to compare physiological indices and relative qRT-PCR expression data ($p < 0.05$).

Results

Changes in the resistance phenotype of kiwifruit treated with SHAM

The appearance and morphology of kiwifruit in the SHAM and CK groups differed at different days postinfection (dpi) (Fig. 1). At 0, 1, 3, and 5 dpi, the lesion diameters in the SHAM and CK groups were 0.30 and 0.30 cm, 0.39 and 0.37 cm, 2.41 and 1.49 cm, and 3.03 and 2.02 cm, respectively. At 0 dpi, the lesion diameters in both kiwifruit groups were in the 0–3 cm

range. However, differences between the two groups increased over time. At 5 dpi, the lesion diameter in the CK group increased to 2.02 cm, whereas that in the SHAM group was 3.03 cm. Thus, the lesion diameter in the SHAM group was 1.02 cm higher than that in the CK group, which further confirmed that SHAM treatment reduced the resistance of kiwifruit to *Botrytis cinerea*. These results indicate that appropriate SHAM treatment can reduce the resistance of kiwifruit to *Botrytis cinerea*.

Transcriptome sequence analysis

Sequencing data statistics

The SHAM-treated kiwifruit was inoculated with *Botrytis cinerea*, and the inoculation was repeated three times at three time points on day 0 (C_0h vs S_0h), day 1 (C_24h vs S_24h), day 3 (C_72h vs S_72h), and day 5 (C_120h vs S_120h). Transcriptome sequencing was performed using the kiwifruit tissue.

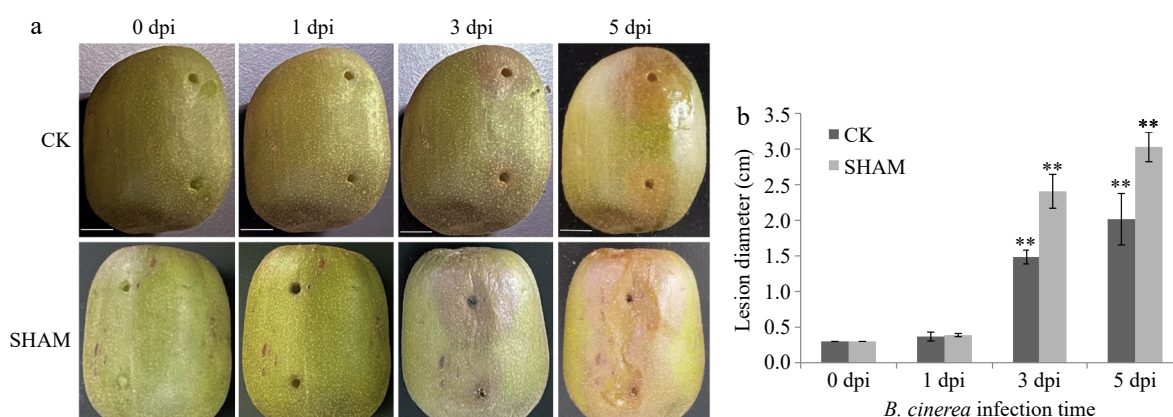


Fig. 1 Changes in the appearance, morphology, and lesion diameter of kiwifruit in the SHAM and CK groups induced by *Botrytis cinerea* at different days postinfection. (a) Changes in the morphological characteristics of kiwifruit at 0, 1, 3, and 5 d post infection (dpi). (b) Changes in the lesion diameter in kiwifruit in the SHAM and CK groups at different time points. *** represents extremely significantly different ($p < 0.01$).

Table 2. Statistics of sequencing data.

Sample name	Raw reads	Raw bases	Clean reads	Clean bases	Error rate	Q20	Q30	GC content
C_0h_1	47524076	7.16G	47391498	7.16G	0.03%	97.65%	93.24%	46.76%
C_0h_2	46500794	7.01G	46365486	7G	0.03%	97.81%	93.62%	46.71%
C_0h_3	40160680	6.05G	40052962	6.05G	0.03%	97.69%	93.27%	46.65%
C_24h_1	42614752	6.42G	42488828	6.42G	0.03%	97.58%	93.05%	46.57%
C_24h_2	43818432	6.6G	43697220	6.6G	0.03%	97.61%	93.09%	46.66%
C_24h_3	39659046	5.98G	39568666	5.97G	0.03%	97.84%	93.61%	46.81%
C_72h_1	39707836	5.98G	39601106	5.98G	0.03%	97.59%	93.07%	46.75%
C_72h_2	39646984	5.98G	39546362	5.97G	0.03%	97.83%	93.63%	46.86%
C_72h_3	40853092	6.16G	40733706	6.15G	0.03%	97.63%	93.18%	46.87%
C_120h_1	38720330	5.83G	38616554	5.83G	0.03%	97.64%	93.17%	47.17%
C_120h_2	45336366	6.83G	45202468	6.83G	0.03%	97.63%	93.15%	46.95%
C_120h_3	42699226	6.43G	42577918	6.43G	0.03%	97.70%	93.31%	46.80%
S_0h_1	47755908	7.2G	47622990	7.19G	0.03%	97.70%	93.31%	46.48%
S_0h_2	45493394	6.85G	45362482	6.85G	0.03%	97.83%	93.63%	46.61%
S_0h_3	42211600	6.36G	42099856	6.36G	0.03%	97.69%	93.28%	46.62%
S_24h_1	44252586	6.67G	44112658	6.66G	0.03%	97.57%	93.04%	46.90%
S_24h_2	38169744	5.75G	38062452	5.75G	0.03%	97.62%	93.15%	46.95%
S_24h_3	38973972	5.87G	38878598	5.87G	0.03%	97.87%	93.72%	47.05%
S_72h_1	44924206	6.77G	44725720	6.75G	0.03%	97.32%	92.49%	47.12%
S_72h_2	41152860	6.2G	41023726	6.19G	0.03%	97.86%	93.72%	47.19%
S_72h_3	40050140	6.04G	39942390	6.03G	0.03%	97.62%	93.14%	46.96%
S_120h_1	37938536	5.72G	37839310	5.71G	0.03%	97.61%	93.12%	47.26%
S_120h_2	42220850	6.36G	42087276	6.36G	0.03%	97.58%	93.15%	47.34%
S_120h_3	42243486	6.36G	42114890	6.36G	0.03%	97.69%	93.37%	47.24%

Table 3. Comparison of rReads and reference sequences.

Sample name	Total reads	Total mapped	Multiple mapped	Uniquely mapped	Read-1	Read-2	Readsmapt0+'	Readsmapt0-'	Non-splicereads	Splicereads
C_0h_1	47391498	44964944 (94.88%)	1713494 (3.62%)	43251450 (91.26%)	21625725 (45.63%)	21625725 (45.63%)	21625725 (45.63%)	21625725 (45.63%)	26448459 (55.81%)	16802991 (35.46%)
C_0h_2	46365486	44059000 (95.03%)	1625332 (3.51%)	42433468 (91.52%)	21216734 (45.76%)	21216734 (45.76%)	21216734 (45.76%)	21216734 (45.76%)	25833515 (55.72%)	16597953 (35.89%)
C_0h_3	40052962	38138198 (95.22%)	1437330 (3.59%)	36700868 (91.63%)	18350434 (45.82%)	18350434 (45.82%)	18350434 (45.82%)	18350434 (45.82%)	22123727 (55.24%)	14577141 (36.39%)
C_24h_1	42488828	39228228 (92.33%)	1541524 (3.63%)	37686704 (88.7%)	18843352 (44.35%)	18843352 (44.35%)	18843352 (44.35%)	18843352 (44.35%)	23334117 (54.92%)	14352587 (33.78%)
C_24h_2	43697220	41131072 (94.13%)	1626420 (3.72%)	39504652 (90.41%)	19752326 (45.2%)	19752326 (45.2%)	19752326 (45.2%)	19752326 (45.2%)	23913823 (54.73%)	15590829 (35.68%)
C_24h_3	39568666	36938290 (93.35%)	1450522 (3.67%)	35487768 (89.69%)	17743884 (44.84%)	17743884 (44.84%)	17743884 (44.84%)	17743884 (44.84%)	21343865 (53.94%)	14143903 (35.75%)
C_72h_1	39601106	37270004 (94.11%)	1464402 (3.7%)	35805602 (90.42%)	17902801 (45.21%)	17902801 (45.21%)	17902801 (45.21%)	17902801 (45.21%)	21764204 (54.96%)	14041398 (35.46%)
C_72h_2	39546362	37400570 (94.57%)	1504068 (3.8%)	35896502 (90.77%)	17948251 (45.39%)	17948251 (45.39%)	17948251 (45.39%)	17948251 (45.39%)	22088098 (55.85%)	13808404 (34.92%)
C_72h_3	40733706	38245790 (93.89%)	1521084 (3.73%)	36724706 (90.16%)	18362353 (45.08%)	18362353 (45.08%)	18362353 (45.08%)	18362353 (45.08%)	22622406 (55.54%)	14102300 (34.62%)
C_120h_1	38616554	33816150 (87.57%)	1574710 (4.08%)	32241440 (83.49%)	16120720 (41.75%)	16120720 (41.75%)	16120720 (41.75%)	16120720 (41.75%)	19925731 (51.6%)	12315709 (31.89%)
C_120h_2	45202468	41753966 (92.37%)	1695002 (3.75%)	40058964 (88.62%)	20029482 (44.31%)	20029482 (44.31%)	20029482 (44.31%)	20029482 (44.31%)	24363679 (53.9%)	15695285 (34.72%)
C_120h_3	42577918	39318158 (92.34%)	1846690 (4.34%)	37471468 (88.01%)	18735734 (44%)	18735734 (44%)	18735734 (44%)	18735734 (44%)	22576173 (53.02%)	14895295 (34.98%)
S_0h_1	47622990	43144188 (90.6%)	1804166 (3.79%)	41340022 (86.81%)	20670011 (43.4%)	20670011 (43.4%)	20670011 (43.4%)	20670011 (43.4%)	25591719 (53.74%)	15748303 (33.07%)
S_0h_2	45362482	41979524 (92.54%)	1554640 (3.43%)	40424884 (89.12%)	20212442 (44.56%)	20212442 (44.56%)	20212442 (44.56%)	20212442 (44.56%)	24638686 (54.32%)	15786198 (34.8%)
S_0h_3	42099856	39315626 (93.39%)	1510886 (3.59%)	37804740 (89.8%)	18902370 (44.9%)	18902370 (44.9%)	18902370 (44.9%)	18902370 (44.9%)	22678429 (53.87%)	15126311 (35.93%)
S_24h_1	44112658	41846144 (94.86%)	1662310 (3.77%)	40183834 (91.09%)	20091917 (45.55%)	20091917 (45.55%)	20091917 (45.55%)	20091917 (45.55%)	24359883 (55.22%)	15823951 (35.87%)
S_24h_2	38062452	36153600 (94.98%)	1412136 (3.71%)	34741464 (91.27%)	17370732 (45.64%)	17370732 (45.64%)	17370732 (45.64%)	17370732 (45.64%)	21234325 (55.79%)	13507139 (35.49%)
S_24h_3	38878598	36883350 (94.87%)	1465624 (3.77%)	35417726 (91.1%)	17708863 (45.55%)	17708863 (45.55%)	17708863 (45.55%)	17708863 (45.55%)	21502098 (55.31%)	13915628 (35.79%)
S_72h_1	44725720	41128472 (91.96%)	1876526 (4.2%)	39252216 (87.76%)	19626108 (43.88%)	19626108 (43.88%)	19626108 (43.88%)	19626108 (43.88%)	24421759 (54.6%)	14830457 (33.16%)
S_72h_2	41023726	38514036 (93.88%)	1702480 (4.15%)	36811556 (89.73%)	18405778 (44.87%)	18405778 (44.87%)	18405778 (44.87%)	18405778 (44.87%)	22568830 (55.01%)	14242726 (34.72%)
S_72h_3	39942390	37195056 (93.12%)	1558874 (3.9%)	35636182 (89.22%)	17818091 (44.61%)	17818091 (44.61%)	17818091 (44.61%)	17818091 (44.61%)	21984331 (55.04%)	13651851 (34.18%)
S_120h_1	37839310	34998938 (92.49%)	1566774 (4.14%)	33432164 (88.25%)	16716082 (44.18%)	16716082 (44.18%)	16716082 (44.18%)	16716082 (44.18%)	20896975 (55.23%)	12535189 (33.13%)
S_120h_2	42087276	38673976 (91.89%)	1863200 (4.43%)	36810776 (87.46%)	18405388 (43.73%)	18405388 (43.73%)	18405388 (43.73%)	18405388 (43.73%)	23284707 (55.32%)	13526069 (32.14%)
S_120h_3	42114890	38897188 (92.36%)	1769032 (4.2%)	37128156 (88.16%)	18564078 (44.08%)	18564078 (44.08%)	18564078 (44.08%)	18564078 (44.08%)	23428900 (55.63%)	13699256 (32.53%)

A total of 24 groups of cDNA libraries were sequenced. The average values for Q20 and Q30 were 97.67% and 93.31%, respectively, indicating a good sequencing quality. Statistics of the sequencing data (such as clean reads and clean bases) and a comparison of clean reads with reference genomes are provided in Tables 2 & 3.

Overall analysis of differentially expressed genes

Transcriptome sequencing revealed 37,159 expressed genes. According to the criteria of FDR < 0.05 and |log₂FC| greater than 1, the DEGs between the SHAM treatment and control groups were identified (Fig. 2). In the S_24h vs S_0h comparison, 714 DEGs were identified, of which 272 genes were downregulated and 442 were upregulated. In the S_72h vs S_0h comparison, 1,511 DEGs were identified, of which 571 were downregulated and 940 were upregulated. A total of 4,181 DEGs were identified in the S_120h vs S_0h comparison, of which 1,448 were downregulated and 2,733 were upregulated. In the S_0h vs C_0h comparison, the number of DEGs (88) was small, the DEGs were not obvious, and the difference between the up- and downregulated genes was small, highlighting the authenticity of these results.

The DEGs were associated with flavonoid biosynthesis (CEY00_Acc08970: chalcone synthase; CEY00_Acc24272: spermidine hydroxycinnamoyl transferase; CEY00_Acc24272: spermidine hydroxycinnamoyl transferase; CEY00_Acc16583: trans-cinnamate 4-monooxygenase; CEY00_Acc01005: dihydroflavonol 4-reductase; and CEY00_Acc32390: flavonoid 3',5'-hydroxylase), phenylpropanoid biosynthesis (CEY00_Acc02578: caffeic acid 3-O-methyltransferase; CEY00_Acc11227: caffeoyl-CoA O-methyltransferase; CEY00_Acc20943: phenylalanine ammonia-lyase; CEY00_Acc02557: 4-coumarate-CoA ligase like; and CEY00_Acc01851: cationic peroxidase), stilbene compound (CEY00_Acc11227: caffeoyl-CoA O-methyltransferase; CEY00_Acc24272: spermidine hydroxycinnamoyl transferase; CEY00_Acc16583: trans-cinnamate 4-monooxygenase; CEY00_Acc07635: spermidine hydroxycinnamoyl transferase; and CEY00_Acc29568: shikimate O-hydroxycinnamoyltransferase), MAPK signal pathways - Plant (CEY00_Acc22367: mitogen-activated protein kinase; CEY00_Acc03023: WRKY transcription factor 33; CEY00_Acc04863: endochitinase; CEY00_Acc20092: nucleoside diphosphate kinase; and CEY00_Acc00618: EIN3-binding F-box protein), plant hormone signal transduction (CEY00_Acc00550), indole-3-acetic acid-amido synthetase (CEY00_Acc24308: transcription factor like; CEY00_Acc00888: xyloglucan endotransglucosylase/hydrolase protein; CEY00_Acc11805: histidine kinase; and CEY00_Acc07445: basic form

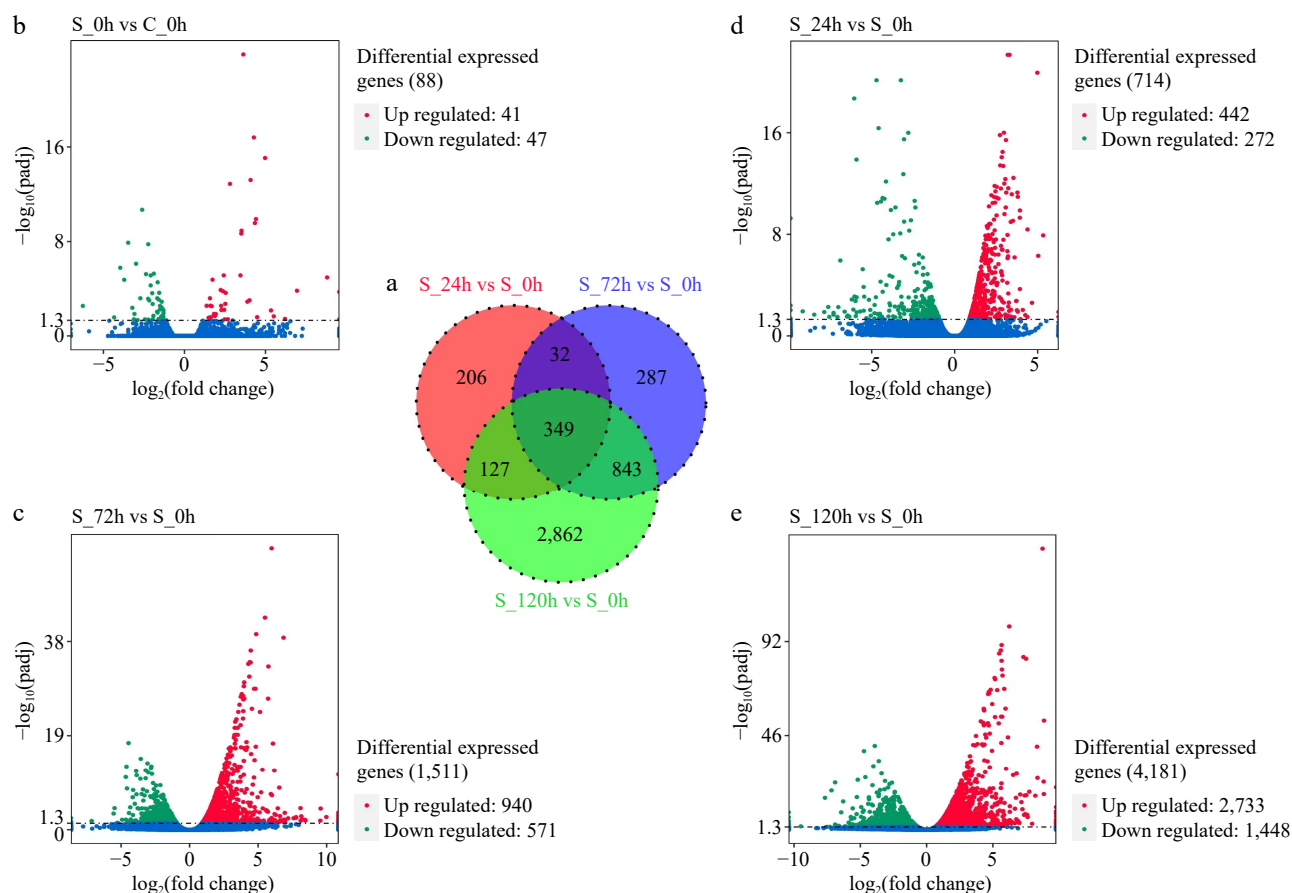


Fig. 2 (a) Venn diagram of differentially expressed genes (DEGs) between different groups (S_24h vs S_0h, S_72h vs S_0h, and S_120h vs S_0h). (b)–(e) Volcano plots of DEGs in different samples. Each dot represents a DEG. Red and green represent significantly up and down-regulated DEGs.

of pathogenesis-related protein endoplasmic like), and plant-pathogen interactions (CEY00_Acc23552: endoplasmic like; CEY00_Acc31880: pathogenesis-related transcriptional activator like; CEY00_Acc19497: disease resistance protein; CEY00_Acc07445: basic form of pathogenesis-related protein like; CEY00_Acc00158: RPM1-interacting protein).

In summary, these results proved that SHAM treatment regulates the resistance response of kiwifruit to *Botrytis cinerea*.

KEGG pathway enrichment analysis of differentially expressed genes

KEGG pathway enrichment analysis of the abovementioned DEGs was performed. In the S_24h vs S_0h_ALL comparison, 16 genes were enriched in the flavonoid biosynthesis pathway, 14 in the MAPK signaling pathway-plant, 10 in cysteine and methionine metabolism pathways, 12 in the starch and sucrose metabolism pathway, 10 in amino sugar and nucleotide sugar metabolism pathways, 19 in plant hormone signal transduction pathways, and four in the pentose phosphate pathway. In the S_72h vs S_0h_ALL comparison, 21 DEGs were enriched in carbon fixation in photosynthetic organisms pathways, 58 in carbon metabolism pathways, 43 in amino acid biosynthesis pathways, 172 in biosynthesis of secondary metabolites pathways, 24 in the propanoate metabolism pathway, 26 in the starch and sucrose metabolism pathway, nine in the pentose phosphate pathway. In the S_120h vs S_0h_ALL comparison,

148 DEGs were enriched in the carbon metabolism pathway, 120 in the biosynthesis of amino acids, 82 in the glycolysis/gluconeogenesis pathway, 48 in carbon fixation in photosynthetic organisms pathways, 52 in the pyruvate metabolism pathway, and 58 in the starch and sucrose metabolism pathway, and significant changes were observed for these pathways. Figure 3 also shows several other pathways with different enrichment factors and Q values, indicating varying degrees of variation in these pathways under the experimental conditions.

KEGG analysis showed that the metabolic pathways 'flavonoid biosynthesis', 'phenylpropane biosynthesis', 'stilbene compounds', 'diarylheptane compounds and gingerol biosynthesis', 'MAPK signaling pathway', 'plant hormone signal transduction', 'Zeatin biosynthesis', and 'plant-pathogen interaction' were highly enriched. Compared with that in the CK group, the expression levels of most of the genes in these pathways in the SHAM120h group were upregulated after infection with *Botrytis cinerea* (Fig. 4).

qRT-PCR validation of transcriptome data

For qRT-PCR validation of the transcriptome data, nine DEGs enriched for plant disease resistance pathways were randomly selected. The trend of qRT-PCR results was consistent with the transcriptome sequencing results, confirming the validity of the latter (Fig. 5).

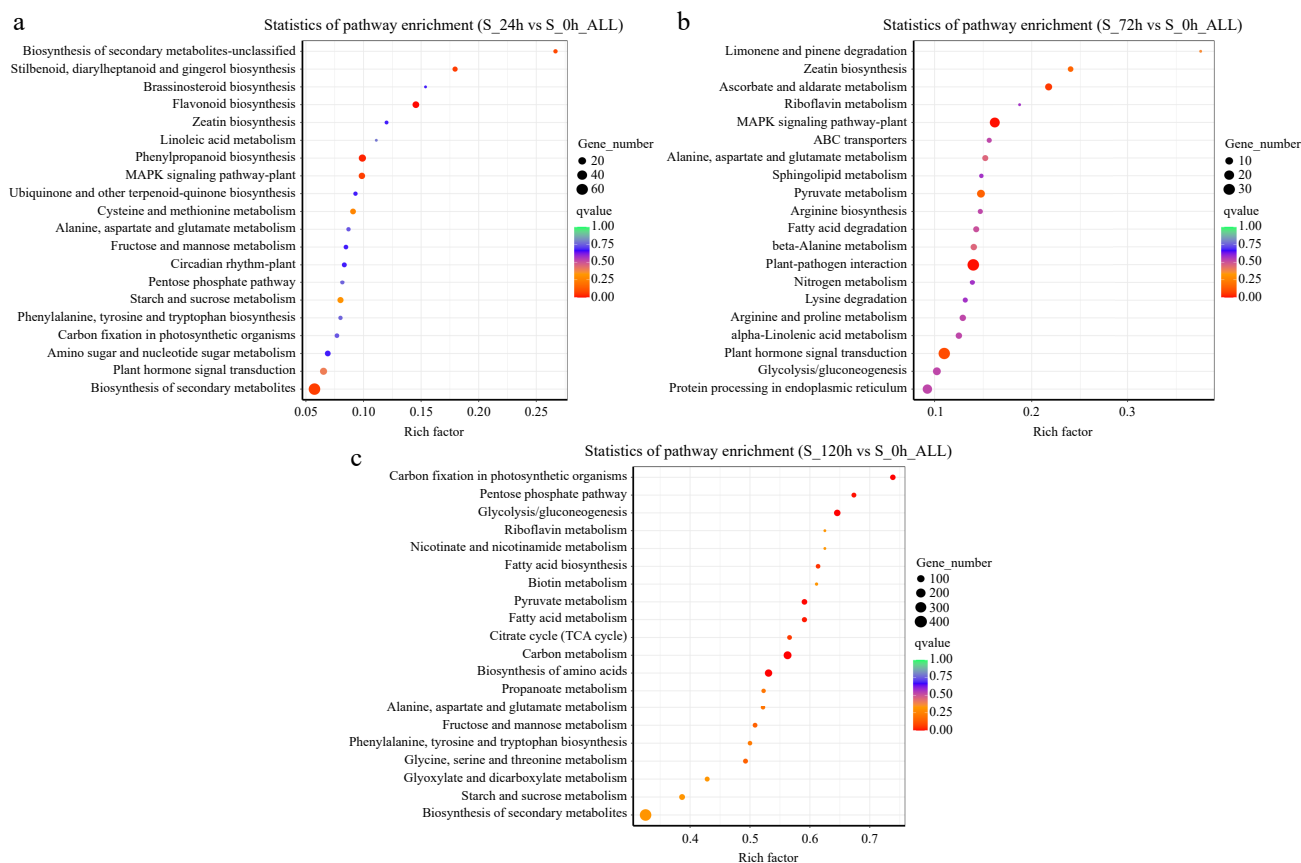


Fig. 3 (a)–(c) Analysis of enriched metabolic pathways in three groups. The top 20 most significant metabolic pathways (based on the p -values) are depicted, with each bubble representing a metabolic pathway. The size of the bubble represents the amount of metabolites in the pathway, as assessed through topological analysis. The color of the bubble represents the p -value of the enrichment analysis (i.e., $-\log_{10} p$ -value); the darker the color, the smaller the p value and the more significant the degree of enrichment.

Discussion

In this study, SHAM treatment of kiwifruit fruit was used to decipher the mechanism of its action in plant disease resistance. Several genes related to key metabolic pathways were found to be differentially regulated by SHAM. These genes can provide a new strategy and scientific basis for the prevention and control of kiwifruit *Botrytis cinerea*. Flavonoid biosynthesis^[19] is the process of conversion of simple precursor molecules, such as the aromatic amino acid phenylalanine, into flavonoids *via* a series of enzyme-catalyzed reactions. Flavonoids play important roles in plant physiology and ecology and are key regulators of plant growth and development, adaptation to the environment, resistance to external pressure, and interaction with other organisms. The MAPK signaling pathway-plant^[20] is an important signal transduction pathway in plants that is involved in the regulation of plant responses to environmental stress, growth, development, interaction, and other biological processes^[21], and is an important mechanism in the adaptation of plants to environmental changes and in their survival. Cys and methionine^[22] play important roles through their involvement in various biological processes, including protein synthesis, antioxidant reactions, sulfur metabolism, and methylation and are crucial for maintaining life activities and normal cell functions. The starch and sucrose metabolic pathway^[23] not only provides the energy and carbon necessary for plant growth but is also an important food source

for humans and animals. The regulation and balance of starch and sucrose metabolic pathways are essential for maintaining normal energy metabolism, growth, and development of organisms. Amino sugar and nucleotide sugar metabolism regulates the formation of cellular structures and cell functions and participates in several important biological processes, such as signal transduction and energy metabolism. Normal metabolism and balance are essential for the proper growth, development, and functional maintenance of cells and organisms. Plant hormone signal transduction is involved in the regulation of physiological processes in plants^[2] and transmission of hormonal signals to the interior of cells, affecting gene expression and metabolic pathways for controlling growth, development, and physiological status. This process involves the synthesis, transport, perception, and signaling of hormones. The pentose phosphate pathway plays important biological roles in cells, including NADPH production, nucleic acid synthesis, and regulation of glucose metabolism, and is critical for normal cellular functions and metabolic regulation. Carbon fixation in photosynthetic organisms^[24] refers to the process of converting inorganic carbon (such as carbon dioxide) into organic compounds through photosynthesis. This process occurs in plants, algae, and some bacteria, and produces organic matter, including glucose, which provides energy and is a source of carbon for living organisms. Carbon metabolism is the process of synthesis, degradation, and transformation of carbon compounds in organisms^[25] that plays an important role in energy generation,

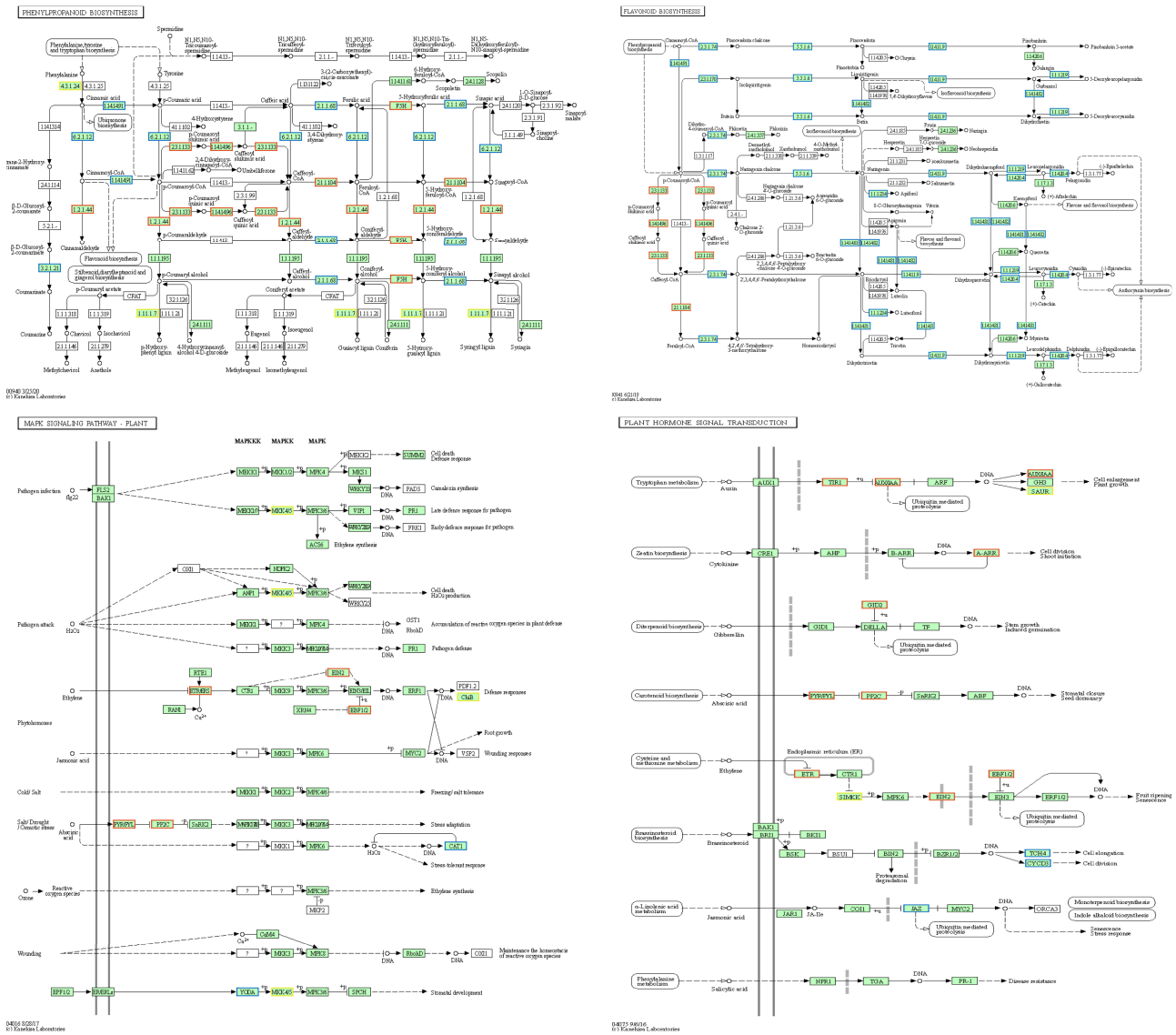


Fig. 4 Diagram showing the important KEGG pathways.

organic synthesis, establishment of cell structures, maintenance of carbon balance, and environmental adaptation. It is an important basis for biological activities. Biosynthesis of amino acids^[26] refers to the biochemical processes of converting simple precursor molecules, such as glycine and pyruvate, into amino acids through a series of enzyme-catalyzed reactions. Amino acid biosynthesis plays important roles in protein synthesis, growth and development, metabolic regulation, stress resistance, and signal transduction and is required for vital activities in organisms. Propanoate metabolism has important physiological and biochemical functions in organisms, including energy production, carbon supply, metabolic regulation, and organic degradation, which are crucial for cell survival and functional maintenance. The biosynthesis of amino acids is essential for cell survival, growth, and function. It not only forms the building blocks of proteins but is also involved in physiological processes, such as regulation of metabolic balance, synthesis of other biomolecules, and provision of energy and carbon sources. Glycolysis and gluconeogenesis are important carbohydrate metabolic pathways responsible for

the breakdown and synthesis of glucose, respectively, for maintaining the stability of cellular energy supply and blood sugar levels. The two pathways interact with each other and together maintain the metabolic balance and physiological functions in the body. Carbon fixation is an important metabolic process in photosynthetic organisms. It supports organic synthesis, cell growth, and division and plays important roles in oxygen production and carbon dioxide reduction, which are crucial for maintaining the stability of the ecosystem and regulating the climate. Pyruvate metabolism is an important metabolic pathway in various organisms. It not only participates in energy production and organic synthesis, but also regulates the redox balance and other metabolic pathways, playing important roles in maintaining cell function and survival.

To conclude, in this study, the role of SHAM, an inhibitor of the JA synthesis pathway, was explored in plant disease resistance, and the potential mechanisms of its action. It was found that to a certain extent, an appropriate concentration of SHAM can reduce the resistance of kiwifruit to *Botrytis cinerea*. To further understand the molecular mechanism behind this

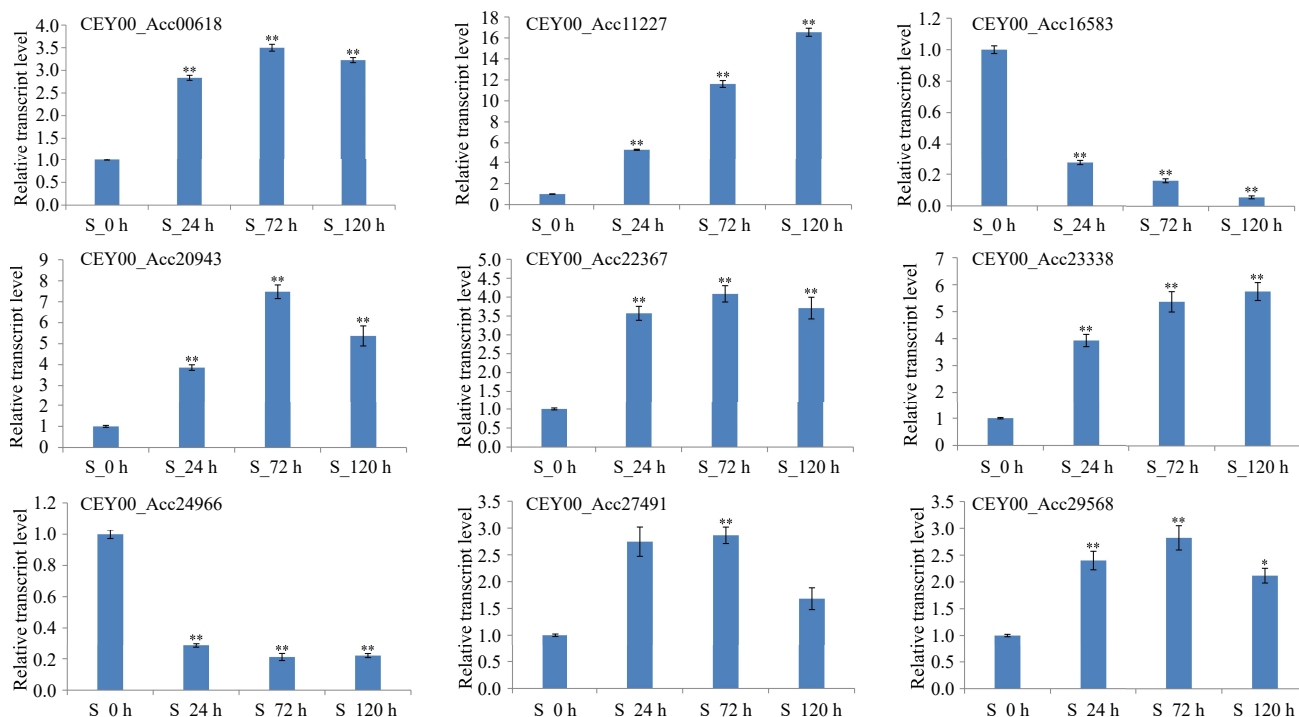


Fig. 5 qRT-PCR analysis of nine genes enriched for plant disease resistance pathways. CEY00_Acc00618: EIN3-binding F-box protein; CEY00_Acc11227: Caffeoyl-CoA O-methyltransferase; CEY00_Acc16583: Trans-cinnamate 4-monooxygenase; CEY00_Acc20943: Phenylalanine ammonia-lyase; CEY00_Acc22367: Mitogen-activated protein kinase; CEY00_Acc23338: Cytokinin dehydrogenase; CEY00_Acc24966: Chalcone synthase; CEY00_Acc27491: Ethylene receptor like; CEY00_Acc29568: Shikimate O-hydroxycinnamoyltransferase. '*' represents significantly different ($p < 0.05$), '**' represents extremely significantly different ($p < 0.01$).

phenomenon, transcriptome sequencing analysis was conducted of fruit materials collected at 0, 24, 48, and 96 h of infection with *Botrytis cinerea* at the junction of disease and health. Using strict statistical screening criteria ($FDR < 0.05$ and $|\log_2FC| > 1$), 714, 1,511, and 4,181 DEGs were identified at the different infection stages. Most of these DEGs were upregulated in SHAM-treated kiwifruit. KEGG pathway enrichment analysis showed that these genes were mainly enriched for metabolic pathways closely related to plant disease resistance, including 'flavonoid biosynthesis', 'Phenylpropane biosynthesis', 'MAPK signaling pathway', and 'plant hormone signal transduction'. These findings not only provide a new perspective for understanding the role of SHAM in enhancing the resistance of kiwifruit to *Botrytis cinerea*, but also provide a scientific basis for devising strategies to control *Botrytis cinerea* in kiwifruit and have practical applicability.

Author contributions

The authors confirm contribution to the paper as follows: study conceptualization: Li Z; methodology: Yang J, Ma Y, Li Z; investigation: Yang J, Ma Y; formal analysis: Yang J, Ma Y, Li Z, Zhang H, Wang X, Zeng T; writing – original draft: Yang J; writing – review & editing, supervision, project administration, funding acquisition: Li Z. All authors reviewed the results and approved the final version of the manuscript.

Data availability

The raw RNA-seq data were deposited in the NCBI SRA database (Accession number: PRJNA1104815).

Acknowledgments

This work was supported by the Natural Science Foundation of Chongqing (CSTB2023NSCQ-MSX0066), and the National Natural Science Foundation of China, China (32001351).

Conflict of interest

The authors declare that they have no conflict of interest.

Dates

Received 20 July 2024; Revised 5 September 2024; Accepted 19 September 2024; Published online 4 November 2024

References

- Thomidis T, Prodromou I, Zambounis A. 2019. Occurrence of *Diaporthe ambigua* Nitschke causing postharvest fruit rot on kiwifruit in Chrysoupoli Kavala, Greece. *Journal of Plant Pathology* 101:1295–96
- Anfang M, Shani E. 2021. Transport mechanisms of plant hormones. *Current Opinion in Plant Biology* 63:102055
- Jodder J. 2020. miRNA-mediated regulation of auxin signaling pathway during plant development and stress responses. *Journal of Biosciences* 45:91
- Monte I. 2023. Jasmonates and salicylic acid: evolution of defense hormones in land plants. *Current Opinion in Plant Biology* 76:102470
- Dai HY, Zhang XK, Bi Y, Chen D, Long XN, et al. 2024. Improvement of *Panax notoginseng* saponin accumulation triggered by methyl jasmonate under arbuscular mycorrhizal fungi. *Frontiers in Plant Science* 15:1360919

Role of methyl Salicylhydroxamic in kiwifruit resistance

6. Deshi V, Homa F, Ghatak A, Aftab MA, Mir H, et al. 2022. Exogenous methyl jasmonate modulates antioxidant activities and delays pericarp browning in litchi. *Physiology and Molecular Biology of Plant* 28(8):1561–69
7. Jeyasri R, Muthuramalingam P, Karthick K, Shin H, Choi SH, et al. 2023. Methyl jasmonate and salicylic acid as powerful elicitors for enhancing the production of secondary metabolites in medicinal plants: an updated review. *Plant Cell, Tissue and Organ Culture (PCTOC)* 153(3):447–58
8. Valenzuela-Riffo F, Zúñiga PE, Morales-Quintana L, Lolas M, Cáceres M, et al. 2020. Priming of defense systems and upregulation of *MYC2* and *JAZ1* genes after *Botrytis cinerea* inoculation in methyl jasmonate-treated strawberry fruits. *Plants* 9(4):447
9. Nakajima N, Inoue H, Koshita Y. 2021. Effects of exogenous methyl jasmonate and light condition on grape berry coloration and endogenous abscisic acid content. *Journal of Pesticide Science* 46(4):322–32
10. He Y, Liu C, Zhu L, Fu M, Sun Y, et al. 2021. Jasmonic acid plays a pivotal role in pollen development and fertility regulation in different types of P(T)GMS rice lines. *International Journal of Molecular Sciences* 22(15):7926
11. Ahammed GJ, Li Z, Chen J, Dong Y, Qu K, et al. 2024. Reactive oxygen species signaling in melatonin-mediated plant stress response. *Plant Physiology and Biochemistry* 207:108398
12. Das P, Agarwala N, Gill SS, Varshney RK. 2023. Emerging role of plant long non coding RNAs (lncRNAs) in salinity stress response. *Plant Stress* 10:100265
13. Noori A, Hasanuzzaman M, Roychowdhury R, Sarraf M, Afzal S, et al. 2024. Silver nanoparticles in plant health: physiological response to phytotoxicity and oxidative stress. *Plant Physiology and Biochemistry* 209:108538
14. Liu T, Xu J, Li J, Hu X. 2019. NO is involved in JA- and H₂O₂ -mediated ALA-induced oxidative stress tolerance at low temperatures in tomato. *Environmental and Experimental Botany* 161:334–43
15. Huguet-Robert V, Sulpice R, Lefort C, Maerskalck V, Emery N, et al. 2003. The suppression of osmoinduced proline response of *Brassica napus* L. var *oleifera* leaf discs by polyunsaturated fatty acids and methyl-jasmonate. *Plant Science* 164(1):119–27
16. Gao X, Yang Q, Minami C, Matsuura H, Kimura A, et al. 2003. Inhibitory effect of salicylhydroxamic acid on theobroxide-induced potato tuber formation. *Plant Science* 165(5):993–99
17. Sircar D, Cardoso HG, Mukherjee C, Mitra A, Arnholdt-Schmitt B. 2012. Alternative oxidase (AOX) and phenolic metabolism in methyl jasmonate-treated hairy root cultures of *Daucus carota* L. *Journal of Plant Physiology* 169(7):657–63
18. Zhou J, Xu Z, Sun H, Zhang H. 2019. Smoke-isolated butenolide elicits tanshinone I production in endophytic fungus *Trichoderma atroviride* D16 from *Salvia miltiorrhiza*. *South African Journal of Botany* 124:1–4
19. Su J, Peng T, Bai M, Bai H, Li H, et al. 2022. Transcriptome and metabolome analyses provide insights into the flavonoid accumulation in peels of *Citrus reticulata* 'Chachi'. *Molecules* 27(19):6476
20. Yan M, Nicolet J. 2023. Specificity models in MAPK cascade signaling. *FEBS Open Bio* 13(7):1177–92
21. Tang J, Wu M, Zhang J, Li G, Yang L. 2021. *Botrytis cinerea* G protein β subunit Bcgb1 controls growth, development and virulence by regulating cAMP signaling and MAPK signaling. *Journal of Fungi* 7(6):431
22. Malle S, Eskandari M, Morrison M, Belzile F. 2020. Genome-wide association identifies several QTLs controlling cysteine and methionine content in soybean seed including some promising candidate genes. *Scientific Reports* 10:21812
23. Yang P, Li Z, Wu C, Luo Y, Li J, et al. 2019. Identification of differentially expressed genes involved in the molecular mechanism of pericarp elongation and differences in sucrose and starch accumulation between vegetable and grain pea (*Pisum sativum* L.). *International Journal of Molecular Science* 20(24):6135
24. Dominguez PG, Niittylä T. 2022. Mobile forms of carbon in trees: metabolism and transport. *Tree Physiology* 42(3):458–87
25. Iqbal A, Dong Q, Wang X, Gui H, Zhang H, et al. 2020. Transcriptome analysis reveals differences in key genes and pathways regulating carbon and nitrogen metabolism in cotton genotypes under N starvation and resupply. *International Journal of Molecular Sciences* 21(4):1500
26. Fang Y, Coulter JA, Wu J, Liu L, Li X, et al. 2021. Identification of differentially expressed genes involved in amino acid and lipid accumulation of winter turnip rape (*Brassica rapa* L.) in response to cold stress. *PLoS One* 16(2):e0245494



Copyright: © 2024 by the author(s). Published by Maximum Academic Press, Fayetteville, GA. This article is an open access article distributed under Creative Commons Attribution License (CC BY 4.0), visit <https://creativecommons.org/licenses/by/4.0/>.